Micromechanical mass sensors for biomolecular detection in a physiological environment

Thomas Braun,* Viola Barwich,* Murali Krishna Ghatkesar,* Adriaan H. Bredekamp, Christoph Gerber, Martin Hegner,†
and
Hans Peter Lang‡

National Center of Competence for Research in Nanoscience, Institute of Physics, University of Basel, 4056 Basel, Switzerland

(Received 1 April 2005; revised manuscript received 19 May 2005; published 14 September 2005)

Micromechanical cantilever arrays are used to measure time-resolved adsorption of tiny masses based on protein-ligand interactions. Here, streptavidin-biotin interactions are investigated in a physiological environment. A measurement method is introduced using higher flexural modes of a silicon cantilever in order to enhance the sensitivity of mass detection. Modeling the cantilever vibration in liquid allows the measurement of absolute mass changes. We show time-resolved mass adsorption of final 7 ± 0.7 ng biotinylated latex beads. The sensitivity obtained is about 2.5 pg/Hz measuring at a center frequency of 750 kHz.

DOI: 10.1103/PhysRevE.72.031907 PACS number(s): 87.83.+a, 68.47.Pe, 87.80.−y, 46.40.−f

I. INTRODUCTION

Proteomic and medical research has a large demand for biosensing tools which allow label-free detection of analytes in real time together with the possibility of massive parallelization of the measurement. In 1994, a new technique based on micromechanical cantilever arrays evolved [1,2]. These developments provided a versatile approach for measuring forces on a nanonewton scale using cantilevers (small springs, with a width and length in the micrometer range but a thickness of 300 nm up to few micrometers). The following changes of physical properties taking place on the cantilever surfaces can be measured, even simultaneously: (1) the surface stress inducing bending of the cantilever (static mode) and (2) the mass load that changes the eigenfrequencies (dynamic mode).

In recent years, it has been demonstrated in static mode that this technique is suitable to detect a single base pair mismatch in DNA hybridization experiments and to compare eight DNA sequences in parallel [3,4] as well as to detect specific cardiac biomarker proteins [5]. In dynamic mode, mass determination of a single airborne virus particle was performed in vacuum [6] and the active growth of microorganisms was measured in real time in humid air [7].

In contrast to other microarray techniques that measure mass adsorption, such as surface plasmon resonance (SPR) detectors [8] and quartz crystal microbalances (QCMs) [9], micromechanical cantilever arrays can be operated in parallel in both static and dynamic modes [10]. Thus mass adsorption and surface stress are measured at the same time. This unique combination of measuring different physical properties simultaneously will allow the design of a new generation of biosensors. We envisage the investigation of membrane proteins in a more sophisticated way. Many of the receptors bind ligands detectable by a mass change in dynamic mode. At the same time they transmit an external signal into the cell, causing conformational changes [11] that are observable in parallel in static mode [12].

Until now, dynamic mode measurements with cantilever arrays were restricted to vacuum or gaseous environments. However, biosensors are required to operate in aqueous solutions. Dynamic mode measurements in fluids still represent a challenge mainly because of the damping of the cantilever oscillation caused by the liquid. Furthermore, fluid is dragged along with the resonating cantilever, resulting in addition of mass to the oscillator and therefore a lowering of the resonance frequency. This is also referred to as "virtual mass" or "virtual mass" [13–16].

In this paper we report time-resolved mass adsorption measurements of biofunctional latex beads in a physiological environment using the biotin-streptavidin interaction. Parallel measurements of this interaction are performed using sensitized and *in situ* negative control reference cantilevers to provide differences in mass responses. Furthermore the proposed theory allows the recording of absolute mass changes on the cantilever in real time.

II. THEORY

Here we present a quantitative description of a cantilever vibrating in liquids for higher modes. The vibration dynamics of a cantilever in vacuum are characterized by the equation of motion, which is given by

$$EI\frac{\partial^4 u(x,t)}{\partial x^4} + C_0\frac{\partial u(x,t)}{\partial t} + \frac{m_c}{L}\frac{\partial^2 u(x,t)}{\partial t^2} = 0. \qquad (1)$$

The first term represents the restoring force per unit length, where EI is the flexural rigidity, with E Young's modulus and I the moment of inertia. C_0 is the intrinsic damping coefficient per unit length that describes internal losses, m_c is the mass of the cantilever, and L is the length of the cantilever. $u(x,t)$ is the deflection of the cantilever perpendicular to the cantilever axis, whereas x is the coordinate along the cantilever axis and t is time.

We focus on cantilevers vibrating in a liquid environment and driven by a piezoelectric crystal plate, which generates

*Spokesperson.
†Author to whom correspondence should be addressed
‡Author to whom correspondence should be addressed. Also at IBM Zurich Research Laboratory, 8803 Rueschlikon, Switzerland.

an external periodic force to the cantilever. In liquid the motion of the cantilever experiences resistance, because not only the cantilever, but also a specific amount of the fluid has to be accelerated. This means that the surrounding fluid acts on the cantilever as if an additional mass m_l were attached to the cantilever. This results in an additional inertial force $g_i = -(m_l/L)\partial^2 u(x,t)/\partial t^2$. The additional mass m_l, or virtual mass, is proportional to the displaced mass of the fluid m_d. This is proportional to the cantilever volume by

$$m_l = p m_d = p \rho_l V_c, \tag{2}$$

where p is a coefficient equal to 1 for an ideal fluid, ρ_l is the density of the liquid, and V_c is the volume of the cantilever [16,17].

In a nonideal fluid an additional dissipative force per unit length acts on the cantilever that is proportional to the velocity, $g_v = -C_v(\partial u(x,t)/\partial t)$, where C_v is the dissipation coefficient. Taking into account the forces g_i and g_v as well as $F(x,t)$, an external periodic force per unit length in Eq. (1), the equation of motion of a cantilever vibrating in liquid is expanded to

$$EI\frac{\partial^4 u(x,t)}{\partial x^4} + (C_0 + C_v)\frac{\partial u(x,t)}{\partial t} + \frac{m_c + m_l}{L}\frac{\partial^2 u(x,t)}{\partial t^2} = F(x,t). \tag{3}$$

In order to solve the problem of a cantilever vibrating in fluid completely, the virtual mass of the liquid m_l and the additional damping force g_v have to be known, i.e., the coefficients p and C_v have to be determined.

Using the deflection $u(t)$, or rather the response of the cantilever, as

$$u(t) = u_0 \exp(i 2\pi f_n t), \tag{4}$$

the resonance frequencies f_n can be determined.

The resonance frequencies of different modes n of the damped cantilever are the complex solutions of Eq. (1), which are as follows:

$$f_n = \frac{1}{2\pi}[\sqrt{\alpha_n^4 (2\pi f_0^*)^2 - \gamma^2} + i\gamma]. \tag{5}$$

The damping factor γ is defined by

$$\gamma = \frac{C_0 + C_v}{(2/L)(m_c + m_l)}. \tag{6}$$

f_0^* is the fundamental eigenfrequency in vacuum when the mass is concentrated in one point as for a harmonic oscillator and in the absence of damping. It is given by the relation

$$f_0^* = \frac{1}{2\pi}\sqrt{\frac{EI}{(m_c + m_l)L^3}} = \frac{1}{2\pi}\sqrt{\frac{k}{3(m_c + m_l)}}, \tag{7}$$

where k is the spring constant given by $k = 3EI/L^3$.

Note that the frequencies of Eq. (5) are identical with the resonance frequencies of a damped harmonic oscillator except for the α_n. The α_n are related to the different eigenvalues of the harmonics and are the nth positive root of the equation $1 + \cos\alpha_n \cosh\alpha_n = 0$ and are fixed by the boundary conditions [18]. [$\alpha_1 = 1.875$, $\alpha_2 = 4.694$, $\alpha_3 = 7.854$, $\alpha_4 = 11.0$, $\alpha_{5,\ldots,n} = \pi(n - 0.5)$.]

For a rectangular cantilever the moment of inertia is $I = WT^3/12$, with W the width and T the thickness of the cantilever. Thus the eigenfrequencies of a cantilever that has a distributed mass in the absence of damping are described in analogy to the model of a harmonic oscillator by

$$f_{0n} = \frac{\alpha_n^2}{2\pi}\sqrt{\frac{k}{3(m_c + m_l)}}. \tag{8}$$

The amplitude of the response of the nth harmonic in dependence on the frequency of the driving force is given according to the model of a damped harmonic oscillator by

$$u_n(f) = \frac{u_{\max} f_{0n}^2}{\sqrt{(f_{0n}^2 - f^2)^2 + \gamma^2 f^2/\pi^2}}. \tag{9}$$

This function is also called the resonance curve and has a maximum at the resonance frequency at

$$f_n = \sqrt{f_{0n}^2 - \frac{\gamma^2}{2\pi}}. \tag{10}$$

Owing to damping effects, the resonance frequency f_n shifts to smaller values with respect to the eigenfrequency f_{0n}. Note that throughout the paper we distinguish between the eigenfrequency f_{0n} defined by Eq. (8) and the resonance frequency f_n defined by the maximum of the amplitude function of Eq. (9), which is specified in Eq. (10). Distinction between these frequencies is important because the eigenfrequency is independent of the damping caused by the liquid whereas the resonance frequency is not.

The phase between response and driving force in dependence on the frequency of the driving force is given by

$$\varphi(f) = \arctan\frac{-\gamma f}{\pi(f_{0n}^2 - f^2)}. \tag{11}$$

The eigenfrequency f_{0n} is defined at that point where the phase curve has its steepest slope. It will be called the turning point of the curve in the following.

In this study we detect an uptake of tiny amounts of mass distributed over the entire cantilever that is due to protein interactions at the interface. Thus the total mass which has to be accelerated is increased by the uniformly loaded mass Δm distributed on the surface of the cantilever:

$$m_{\text{total}} = m_c + m_l + \Delta m. \tag{12}$$

Assuming that the spring constant does not change, the eigenfrequency f_{0n} of Eq. (8) is modified as

$$f'_{0n} = \frac{\alpha_n^2}{2\pi}\sqrt{\frac{k}{3(m_c + m_l + \Delta m)}}. \tag{13}$$

For $\Delta m \ll m_c + m_l$ the following approximation is valid:

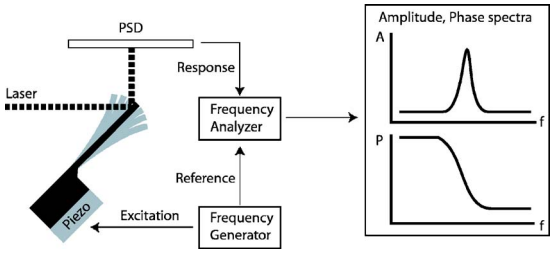

FIG. 1. (Color online) Schematic of the setup. A frequency generator sweeps the spectrum by exciting a piezoelectric actuator located beneath the base of the microcantilever array. The response of the cantilever is optically detected with a laser using a position-sensitive detector. The frequency analyzer compares the cantilever response with the excitation from the frequency generator to determine the phase. The amplitude spectrum is recorded with the corresponding phase values.

$$f'_{0n} \approx f_{0n}\left(1 - \frac{1}{2}\frac{\Delta m}{m_c + m_l}\right). \tag{14}$$

The mass load Δm in terms of the frequency shift Δf is calculated as

$$\Delta m = \frac{2(m_c + m_l)\Delta f}{f_{0n}}, \tag{15}$$

where $\Delta f = f_{0n} - f'_{0n}$.

The sensitivity of a mass-loaded cantilever is defined as

$$S = \frac{\Delta f}{\Delta m} = \frac{f_{0n}}{2(m_c + m_l)}, \tag{16}$$

indicating that the sensitivity increases with the order of the harmonic of the cantilever vibration.

III. EXPERIMENTAL DETAILS

Microfabricated (Micro- and Nanofabrication group, IBM Zurich Research Labratory, Rueschlikon, Switzerland) arrays of eight silicon cantilevers of 500 μm length, 100 μm width, 1 μm thickness, and having a spring constant of 0.03 N/m were used in all the experiments.

A. Measurement setup

A schematic of the setup is shown in Fig. 1. The array with the functionalized cantilevers is directly mounted onto the piezoelectric actuator, which is excited periodically by a frequency generator. The cantilever response is read out using a beam-deflection system: The beam of a vertical cavity surface-emitting laser (wavelength 760 nm, Avalon Photonics, Zurich, Switzerland) is reflected at the tip of the cantilever toward a position-sensitive detector (PSD; Sitek Partille, Sweden).

The response of the cantilever is continuously compared with the excitation using a frequency analyzer recording amplitude and phase spectrum (Hewlett Packard, 4589A, USA). Depending on the number of cantilevers used, a spectrum is recorded every 23 s (one cantilever) or at least every 3 min (parallel measurement of all eight cantilevers). In both configurations, a sweep time of 1 s per spectrum was used. The entire setup is placed in an analysis chamber (volume $\sim$5 μl) which is kept at constant temperature (accuracy $\pm$0.02 K) during the experiment. A constant fluid flow rate in the cell was maintained using a syringe pump (Genie Kent, Indulab AG, Switzerland) or with a pressure driven pump system as described [19].

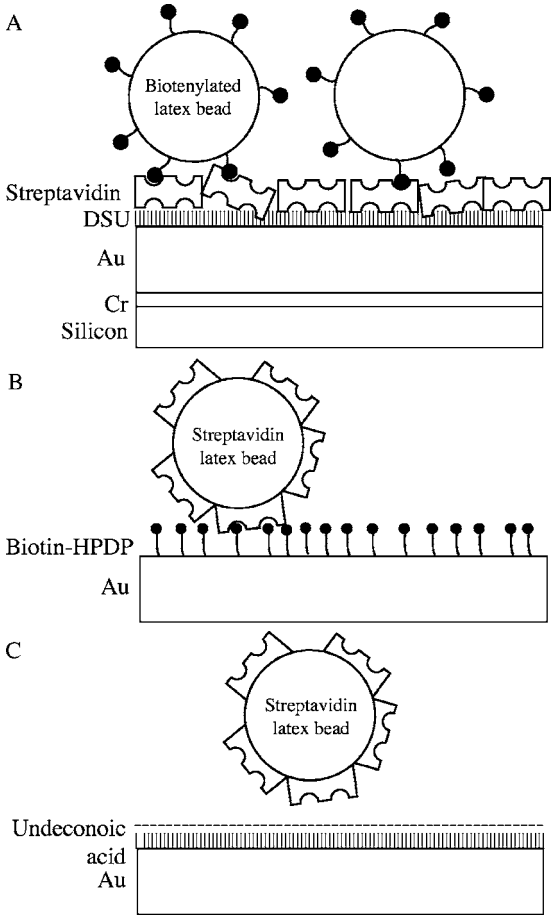

FIG. 2. Schematics of the functionalization methods used. Note that the silicon cantilever and the chrome adhesion layer are only shown in (a). All binding assays are based on streptavidinbiotin-interaction. (a) The gold-coated cantilever was activated with DSU cross-linker, which binds to the gold via a thiol group and reacts by a succimidyl reaction with lysine groups of the protein. (b) Positive functionalization for the binding of streptavidin-coated latex beads with biotin-HPDP. (c) Functionalization of the cantilever with an acid as negative control: At *p*H 8.0 most acid residues are negatively charged, thus repelling the sulfonate-activated latex beads by electrostatic forces.

B. Cantilever functionalization

Piranha-cleaned (30% H_2O_2:H_2SO_4=1:1) arrays were coated with a 2 nm chromium adhesion layer followed by 30 nm gold by sputtering (Baltec SCD 050 for Cr) (120 mA, 0.05 mbar); Baltec MED 020 for Au (50 mA, 0.02 mbar) on both sides. Cantilever arrays were functionalized in two ways (Fig. 2.) using a capillary device described elsewhere [20].

(1) Avidin-functionalized cantilevers were used to bind biotinylated latex beads: On gold-coated cantilevers, homemade cross-linker dithiobis succinimidyl undecanoate (DSU) [21,22] was used to immobilize avidin. The cross-linker formed a monolayer on the cantilever gold surface via the thiol group, and avidin was subsequently immobilized by a succimidyl group protein-lysine reaction; see Fig. 2(a).

(2) Cantilevers were functionalized with a biotin layer to bind streptavidin-coated latex beads. The freshly gold coated cantilever was incubated in an *N*,*N*-dimethylformamide (DMF) solution containing 1 m*M* biotin-HPDP (*N*-[6 -(Biotinamido)hexyl]-3′-(2′-pyridyldithio)propionamide; Perbio Science, Switzerland) for 20 min at room temperature. For a negative control, alternating cantilevers were functionalized during 20 min at room temperature with 1 m*M* 11-mercaptoundecanoicacid (Sigma-Aldrich Inc., Switzerland) in DMF [Fig. 2(b) and 2(c)].

C. Binding assay

For avidin-functionalized cantilevers a buffer solution containing 20 m*M* KPO_4 of *p*H 7.4, 100 m*M* NaCl, and 0.01% NaN_3 was used during the experiment. The density ρ_f and the viscosity η_f were determined to be 1033 kg/m^3 and 9.28×10^{-4} kg m^{-1} s^{-1}, respectively. The carboxylate-modified biotin-labeled polystyrene latex-bead suspension (Sigma-Aldrich, Inc., Switzerland) exhibiting a mean bead diameter of 250 nm was first resuspended, then diluted in the buffer described above to a final bead concentration of 6.5 p*M* and sonicated for 1 min.

For biotin-functionalized cantilevers, a buffer of 10 m*M* HEPES [4-(2-hydroxylethyl)-1-piperazine ethansulfonic acid] *p*H 8.0, 100 m*M* NaCl, 0.01% NaN_3, 0.25 mg/ml casein, and 0.05% tween-20 was used during the experiment. The carboxylate-modified and streptavidin-functionalized beads (Sigma-Aldrich, Switzerland) had an avarage diameter of 47 nm. During these experiments the same mass concentration and preparation as with the first binding experiments (biotin beads) and a final bead concentration of 1 n*M* were applied.

After the binding experiment, the cantilever array was removed from the fluid cell, washed in water to prevent salt-crystal artifacts, coated with 5 nm Pt by sputtering (Baltec, MED 020; 15 mA, 0.02 mbar) and analyzed by scanning electron microscopy (SEM, Phillips XL-30). The SEM images were analyzed with the standard particle analysis software of IGOR PRO (Wavemetrics, Portland, USA).

D. Data analysis

All data-processing algorithms were implemented in the IGOR PRO data analyze environment. Recorded time series of spectra were analyzed using two methods.

(1) Amplitude peak tracking and phase-turning point tracking [23]. Here, the amplitude-peak maximum (resonance frequency) and the phase-turning point (eigenfrequency) were extracted and plotted versus the time. Note that in this method all resonance peaks and phase-turning points were analyzed separately. To minimize noise, the raw data were locally described with a Gauss function (amplitude information) or a sigmoidal function (phase information). Smoothing functions and the raw data matched well.

(2) Least mean square fitting of the spectrum. This method involved the fitting of the amplitude and of the corresponding phase spectrum by the model described in Sec. II. With this method, the complete spectrum was analyzed at once.

The fit function of the resonance peak of an amplitude spectrum was based on the amplitude response function $u(f)$ of Eq. (9). The eigenfrequencies were determined by fitting the phase spectrum with Eq. (11). For spectra exhibiting several peaks, a superposition of peaks or phase transitions was fitted to the complete spectra.

To determine the absolute adsorbed mass during the injection of latex beads, the system had to be calibrated. This means, initially, each spectrum acquired during the first injection step with buffer only was fitted, and various parameters were extracted for each mode. These were the eigenfrequency f_{0n}, the maximum amplitude $u_{\max}$, the sum of the damping constants C_0+C_L, the virtual liquid mass m_l, and a phase shift in the phase spectrum. The latter is a frequency-dependent term taking a constant latency in electronic transmission of the signal into account.

In a next step, the adsorbed mass Δm was fitted for the next two injection sequences including bioreactive polystyrene beads. This was done by keeping the accelerated liquid mass constant by using the calibration from the first fit. The eigenfrequency, the maximum amplitude, and the sum of the damping constants were fitted again.

IV. RESULTS

A. System characterization

System characterization is necessary to determine the absolute mass adsorbed in a subsequent binding experiment. This procedure is presented in Sec. IV B 2. The amplitude spectra are recorded continuously together with the corresponding phase spectra. A typical spectrum including three peaks (modes 11 to 13) is shown in Fig. 3 with a thick gray line.

The resonance and eigenfrequencies were determined by tracking the amplitude peaks and the phase-turning points (Sec. III D). The stability of the tracked frequencies was better than 0.03% over time; for a more detailed discussion see Sec. IV B. To exclude torsional mode peaks, the square root of the eigenfrequency was plotted in dependence of the peak number. The linear relation is a indication that no torsional mode peak is included in the spectrum, Eq. (8).

To compare the data with the model described in Sec. II, the data were fitted with the model. The following parameters were determined: for the amplitude as well as for the phase spectrum the virtual mass of the comoving liquid and the damping factor were fitted for each mode. For the amplitude spectra, the amplitude of the peak was also fitted. For the phase spectra an additional frequency-dependent term, which takes the latency of electronics and cables into account, was introduced. Figure 3 shows the excellent agreement between the measured data and the fit (thin black line).

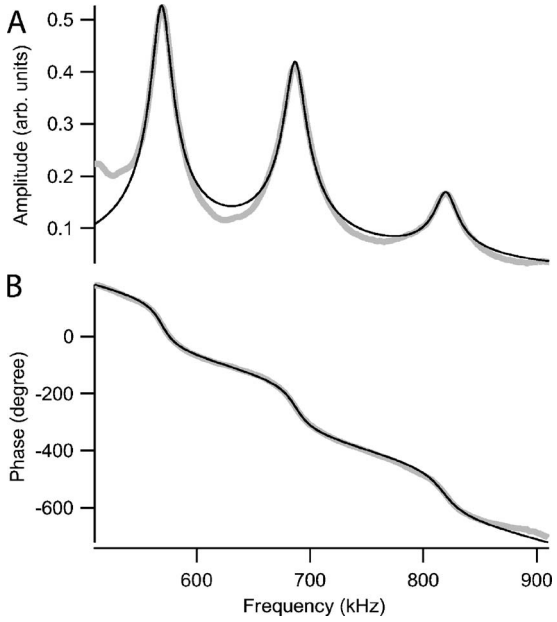

FIG. 3. Amplitude spectra (a) with corresponding phases (b). The raw data are shown in gray, the model fitting as thin black lines. The model is described in detail Sec. II.

In terms of cantilever volumes Eq. (2) the measured volume of the virtual mass corresponded to 15.9 for the 11th, to 15.7 for the 12th, and to 15.4 for the 13th mode. The measured constants for the virtual mass represent some of the physical properties that characterize the system.

The damping factors C_0+C_v are dependent on the virtual mass (including the virtual mass of the dragged liquid), and vary from 1.05×10^{-4} to 1.66×10^{-4} kg/s.

B. Binding assays

Two adsorption reactions were tested: (1) the adsorption of biotinylated latex beads (diameter 250 nm) on streptavidin-activated cantilevers, and (2) the adsorption of streptavidin-coated latex beads (diameter 47 nm) on biotinylated cantilevers (Sec. IV B 3).

The first adsorption experiment was performed in three injection steps of 45 min each: first, injection of buffer, then the same buffer with biotinylated latex beads at a concentration of 6.5 pM, and finally buffer again. A constant flow rate of 17 μl/min was maintained throughout the experiment, keeping the concentration of latex beads constant. The amplitude and phase spectra were recorded every 23 s.

A time-resolved plot of the frequencies is shown in Fig. 4 for all three modes. The eigenfrequencies are indicated by white circles (turning-point tracking of the phase information) and the resonance frequencies by black squares (peak tracking of the amplitude information). The bottom graph shows the time evolution of the frequencies of the 11th, the middle one of the 12th, and the top one of the 13th vibration mode. According to the three steps of injection, each plot consists of three sections of about 45 min.

The plot shows that the eigenfrequencies were found to be at higher values than the resonance frequencies. The eigenfrequencies have been observed to have an average fluctuation of ±130 Hz, whereas the resonance frequencies vary by ±180 Hz in the section before the beads were injected. This means within these 45 min the stability of the eigenfrequency was 0.015% and that of the resonance frequency 0.025%.

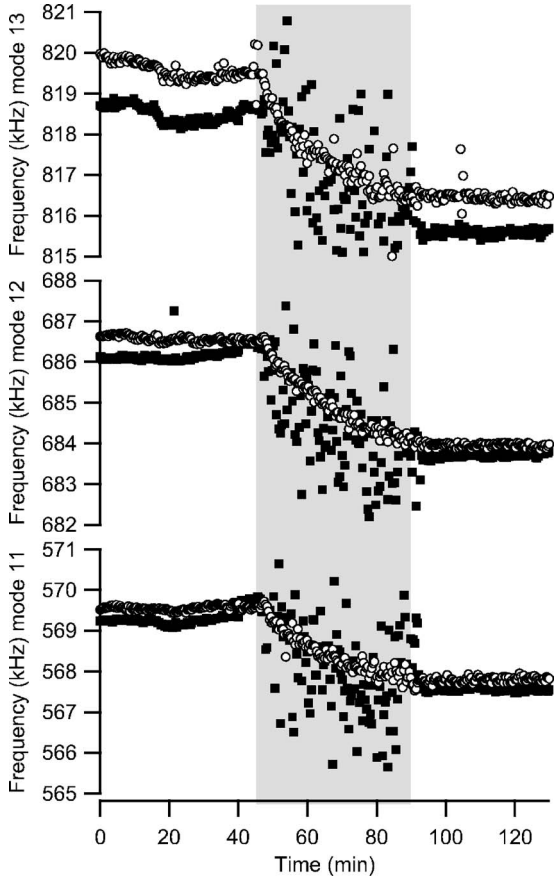

FIG. 4. Change of eigenfrequency (white circles) and resonance frequency (black squares) during adsorption of biotinylated latex beads. The injection time of the beads is indicated by the gray area. The panels from the bottom to top show the time evolution for the 11th, 12th, and 13th modes. Note that the frequency shift increases with higher modes upon latex-bead injection. Furthermore the resonance frequencies are significantly scattered during this time whereas the eigenfrequencies are recorded smoothly.

The injection of latex beads suspension is indicated by a gray area (Fig. 4). During this period, simultaneously with the injection of latex-bead suspension, the frequencies shifted monotonously to smaller values. The trend in the plot of eigenfrequencies exhibited an exponential saturation behavior which was explained by the binding of latex beads to the cantilever, thus successively occupying free binding sites. In contrast to the eigenfrequencies, the resonance frequencies scattered to a large extent during the time of latex-bead injection.

In the last section, while the fluid cell was flushed with buffer, the resonance frequencies became stable again, immediately exhibiting average fluctuations of ±59 Hz. The stability of the eigenfrequencies was ±103 Hz. The data reveal a stability of 0.015% for the eigenfrequency and of ap-

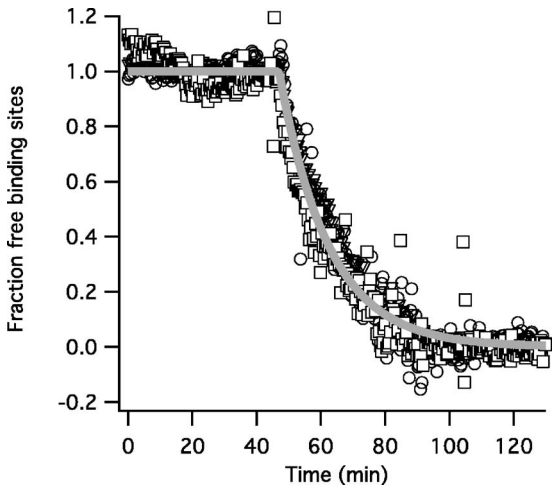

FIG. 5. Comparison of the frequency shifts upon mass load for different modes. The raw data of the frequency shifts have been normalized and represent the fraction of the free binding sites assuming that the cantilever is fully saturated with latex beads at the end of the experiment. Circles, mode 11; triangles, mode 12; squares, mode 13. A pseudo-first-order kinetic model was fitted to the data (thick gray line).

proximately 0.010% for the resonance frequency within this time period.

The permanent decrease in the frequency after bead binding and flushing the fluid cell with buffer indicates that the latex beads were irreversibly bound to the cantilever surface, generating a mass load on the cantilever.

In total, the eigenfrequencies shifted by −1555 Hz from 569 561 Hz for the 11th mode, by −2419 Hz from 686 571 Hz for the 12th mode, and by −3130 Hz from 819 575 Hz for the 13th mode. Correspondingly, the resonance frequencies shifted by −1689 Hz from 569 296 Hz for the 11th mode, by −2761 Hz from 686 166 Hz for the 12th mode, and by −2814 Hz from 818 507 Hz for the 13th mode.

1. Kinetic model

To compare the three time-resolved measurements shown in Fig. 4 with each other, the eigenfrequencies were normalized for all three measured modes (Fig. 5).

The overlay of the three time-dependent curves confirms the equivalence of the information independent of the vibrational mode used. The normalized data are interpreted as contribution of the gradual coverage of the free biotin binding sites of the streptavidin functionalization on the cantilever during injection of latex beads. To further analyze the data, a pseudo-first-order model was fitted assuming the following. (1) The concentration of the latex beads is constant as we pump the beads through the measurement chamber. (2) The beads bind irreversibly to the cantilever. (3) The binding sites on the cantilever are all occupied after 45 min at the end of the experiment. Therefore the binding rate of the latex beads is proportional to the free binding sites, and the bead concentration is part of the rate constant. Consequently, a single parameter exponential decay, $B_{\text{free}}=B_0e^{-\tau t}$, was fitted to the average of the normalized binding curves. An adsorption rate of $\tau=0.06\ \text{min}^{-1}$ was measured. The concentration-independent rate constant is $\tau^*=9.23\times10^9\ M^{-1}\ \text{min}^{-1}$.

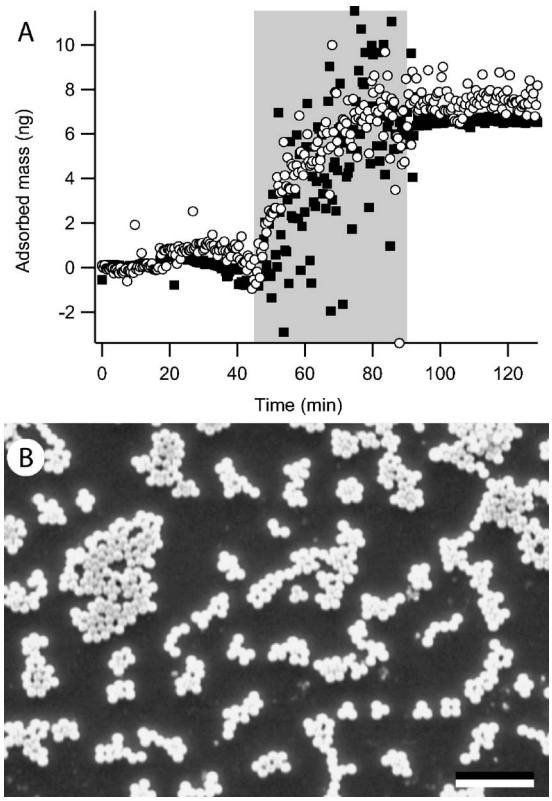

FIG. 6. (a) Absolute adsorbed mass determined by fitting the model to the phase information (white circles) and the amplitude spectrum (black squares). The gray area indicates the time frame of latex-bead injection. At the beginning of the experiment, the virtual mass was determined with the first spectrum of the experiment. Note that every point corresponds to a fit of a complete amplitude or phase spectrum including modes 11–13. (b) Scanning electron micrograph of a typical cantilever covered with latex beads (diameter 250 nm) after experiment. The scale bar corresponds to 2 μm.

2. Absolute mass calculation

Each spectrum of the time series of phase and amplitude spectra was fitted using the model described in Sec. IV A. For the calculation of the absolute mass, the previously determined virtual mass is kept constant, but an additional mass term for the adsorbed mass is fitted, Eq. (12). The time-resolved absolute-mass increase during latex-bead adsorption on the cantilever is shown in Fig. 6(a). The trend of the two curves obtained from the amplitude fits and from the phase fits is similar: a mass adsorption of 7±0.7 ng beads was measured as extracted from the fits of the phase information. However, the increase of the mass for the phase fit is ~0.7 ng larger than that for the amplitude fit.

The estimated number of beads of the adsorbed mass is 8 beads per μm^2, assuming a bead density of 1050 kg/m^3, and a bead diameter of 250 nm.

After the experiment, the cantilever was removed from the fluid chamber, dried, coated with 5 nm Pt, and imaged in the SEM. The particles were counted, yielding a coverage of

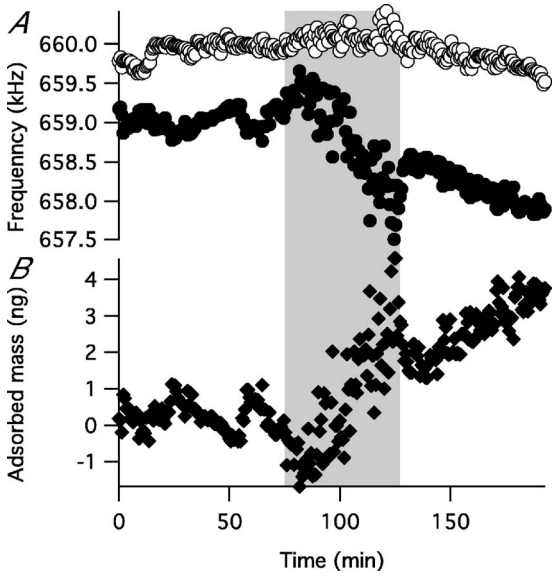

FIG. 7. Parallel and differential adsorption measurement of streptavidin-coated beads. (a) Change of eigenfrequency during streptavidin adsorption. Injection of beads is indicated by the gray area. Time evolution of the eigenfrequency extracted from the turning point of the phase. Black circles, eigenfrequency of the biotin-functionalized cantilever. White circles, eigenfrequency of a blocked cantilever. (b) Absolute mass adsorbed on the cantilever measured by fitting the phase information of (a) with the model.

4 particles per μm^2 on average in different experiments. However, bead counting using SEM images was not very reproducible because shear forces often caused washing effects [24] during sample preparation for the SEM: coating with latex beads was not homogeneous. We observed areas without any beads surrounded by areas with very high bead densities, followed again by an average bead density. Furthermore, the counting algorithm tends to underestimate the beads on a cantilever as beads sitting on top of each other are not counted, but have regularly been observed in the images.

3. Differential measurement

The second adsorption experiment was performed analogously to the first adsorption experiment but with smaller (47 nm) strepavidin-coated beads, using sensor and reference cantilevers: The sensor cantilever was functionalized with biotin [Fig. 2(b)] and the negative control (reference lever) with an acid [11-thio-undecanoic acid, Fig. 2(c)] introducing a negative charge on the cantilever repelling negatively charged latex beads.

The measurements revealed a clear decrease of the eigenfrequency of the biotin-functionalized cantilever of 550 Hz compared with the nonmeasurable shift of the control cantilever (Fig. 7). Note that both cantilever eigenfrequencies were read out in parallel from the cantilever array and that the measurement was done in the presence of another protein (0.25 mg/ml casein) and detergent (0.05% tween-20). In addition, the corresponding mass increase was determined by fitting the model to the phase information obtained from the sensitized cantilever. The mass increase on the cantilever exhibits the same qualitative behavior as the turning point tracking method. A mass increase of 1.66 ± 0.564 μg was observed.

V. DISCUSSION

Here we describe experiments to measure mass adsorption under physiological conditions in real time. Two methods were used to analyze the time-series of recorded spectra (Fig. 1): The first method reads out resonance and eigenfrequencies (method 1, Sec. III D), the second determines the absolute adsorbed mass (method 2).

The analysis of the frequency in dependence on time (method 1) revealed a clear shift to lower frequencies upon latex-bead adsorption. A clear and exponential decay of the eigenfrequencies immediately after bead injection was observed following a saturation behavior. This was seen by a shift in eigenfrequency and resonance frequency (Fig. 4). Thereby, three phenomena were observed. (1) The frequency shift upon mass binding increased for higher modes. (2) The values of the eigenfrequency (determined from the phase data) were higher than those of the resonance frequency (determined from the maximum peak amplitude). (3) During bead injection, the resonance frequencies from the amplitude information scattered significantly, whereas the eigenfrequencies obtained from phase information were recorded smoothly.

Phenomenon 1 confirmed Eq. (16), which describes the enhanced mass sensitivity of cantilever vibrations at higher modes. Phenomenon 2 proved Eq. (10), namely, that the damping shifts the resonance frequencies to lower values with respect to the eigenfrequencies, which are independent of damping. The last phenomenon, the scattering of the resonance frequencies, was due to significant noise in the amplitude spectra during bead injection. This was interpreted as a rapid change of the external damping C_v during the 1-s-long sweep of the spectrum. The damping fluctuation was due to the change of the interaction of the cantilever with the surrounding medium, in our case, the collisions of the 250 nm latex beads with the 1-μm-thick cantilever resulting in a higher noise level. This observation is completely described by the theory (see Sec. II). Therefore we conclude that the eigenfrequencies should be measured instead of resonance frequencies to obtain a better signal to noise ratio.

Normalization of the extracted frequency changes revealed clearly that the information obtained at different modes is equivalent (Fig. 5). Therefore an evaluation of more than one peak minimizes the error of the data interpretation (fraction of binding sites, mass-adsorption determination).

To determine the adsorbed mass (method 2), the virtual mass of the liquid has to be considered. This was done by a least mean square fit of the phase and amplitude data before the latex beads were injected. For every mode, the virtual mass was determined in terms of cantilever volumes: Values between 15 and 16 have been found. In other words, when using a 1-μm-thick cantilever, an apparent layer of 7 to 8 μm of water with a mass of ~ 80 μg is moved along with the cantilever.

We assume that during the latex-bead experiment, the thickness of the water layer is not changed because the mol-

ecules or the latex beads, are much smaller and the measured virtual mass m_l is much larger than the adsorbed mass Δm. This allows a direct tracking of newly and gradually adsorbed mass by fitting the phase spectra while keeping the virtual mass of the water constant.

In general not only the adsorbed particle contributes to the mass load of the cantilever, but also the structural water molecules bound to the particle will contribute to the mass increase. As we already took a thick water shell of the virtual mass into account, we assume that the particle-bound water simply substitutes the water molecules of the virtual mass and is already included in the initial calibration before bead injection. Therefore we are able to determine the net mass of the particles.

The limitations of our model are the assumptions that the binding mass is distributed homogeneously along the entire cantilever and that the cantilever is perfectly rectangular-shaped. Furthermore we assume that the cantilever spring constant k does not change throughout the experiment. Intuitively, at a complete coverage of the cantilever surface with the analyte, the spring constant k might increase, which means that the cantilever gets stiffer.

The development of the mass increase in time displayed in Fig. 6 (method 2) shows the same qualitative behavior as do the changes of the eigenfrequencies (method 1) observed during latex-bead adsorption, Fig. 4. As expected the masses determined from the amplitude information scattered more during latex-bead injection (see discussion above). Furthermore, the final mass differs by -0.7 ng ($\sim 10\%$) when extracted from the amplitude information rather than from for the phase data. This can be explained by the fact that the damping factor also varies during the fitting of the amplitude information: The shift of the resonance frequency can be interpreted as an increase in mass but also in damping. Therefore fitting the amplitude information tends to overestimate damping and underestimate adsorbed mass.

The number of latex beads as counted from the SEM images of the cantilever used and the estimated adsorbed mass thereof corroborate the mass determined by method 2. This is also in good agreement with calculations for the maximum possible number of binding sites on the cantilever assuming a perfect hexagonal arrangement (1.85×10^6 beads/cantilever). Compared with our data, this means that 45% of the cantilever was covered with beads.

Combining the kinetic model evaluating the eigenfrequencies (method 1) with the absolute mass evaluation (method 2) allows a further level of quantitative data analysis for biological reaction. The number of adsorbed beads can be calculated (8.58×10^5 for the entire cantilever). Thus, absolute rates (number of beads) adsorbing to the cantilever for every point in time during the adsorption experiment can be given.

We presented also the differential measurement between positive and negative control functionalized cantilevers in a complex mixture of latex beads (47 nm in diameter), protein (0.25 mg/ml casein) and detergent (0.05% tween-20), see Fig. 7. These data demonstrate the potential of our technique for massive parallelization and real-time measurements with high precision to measure absolute masses. High-density two-dimensional arrays of cantilevers already have been presented [25], and there is in principle nothing that would preclude going even to three-dimensional cantilever-array stacks.

The sensitivity of our technique is 220 to 400 Hz/ng, depending on the oscillation mode measured, Eq. (16). This corresponds to a sensitivity of 2.5 pg/Hz at a center frequency of about 750 kHz. The sensitivity of our measurements (Fig. 6) per sensor area is 70 fg/μm^2 or 0.025 fg/μm^2 Hz, taking into account the double-sided functionalization of the cantilever. Furthermore we detected latex-bead particles in the low picomolar range in a 5 μl analysis chamber.

As an outlook, we expect a resolution in the frequency range of 0.01 Hz, as reported earlier using a phase-locked loop system (PLL) [26]. This would correspond to a mass resolution of 25 fg or 0.25 ag/μm^2, using a PLL operating at around 750 kHz. The resolution can also be increased if the measurements are done at higher frequencies. Using a PLL would also increase the resolution in time: As the damping in the system is high, a fast tracking in the millihertz range should be feasible. For measurements of the absolute mass, the frequency changes recorded in this way can be calibrated by the method described above (method 2).

It is interesting to compare our data with the sensitivity and resolution of other micro-array techniques such as surface plasmon resonance imaging and quartz microbalance techniques. A direct comparison with QCM, thus measuring frequency shifts, is possible: A recent publication [27] described a sensitivity of 0.17 fg/μm^2 Hz measured at frequencies of up to 35 MHz under physiological conditions. For SPR, a comparison is more difficult because different physical properties are measured than in our technique and there is no absolute relation between the measured signal and the adsorbed mass. The resolution of SPR in general is supposed to be around 1 ag/μm^2 [28].

VI. CONCLUSIONS

A simple and efficient technique is proposed to measure time-resolved mass adsorption independent of the chemical nature of the adsorbant. The absolute bound mass could be measured at a sensitivity of 2.5 pg/Hz at a center frequency around 750 kHz. This microarray technique combines a potential high-throughput screening method with high-precision mass measurement under physiological conditions. The expected resolution is comparable to or even better than that of SPR, and the sensitivity is better than that obtained in optimized QCM measurements. Measuring at higher frequencies will further improve sensitivity and mass resolution. Furthermore, measuring in combination with other nanomechanical property changes such as surface stress (combination with static mode), [10] an even more advanced level of sensitivity and resolution can be achieved. Such a tool will be especially useful to measure membrane-protein ligand interactions.

ACKNOWLEDGMENTS

We thank Marko Dorrestijn (IBM Zurich Research Laboratory, Rueschlikon, Switzerland), Felice Battiston (Concen-

tris GmbH, Basel, Switzerland), and Andreas Engel (Biozentrum, University of Basel, Switzerland) for fruitful discussions. Financial support is acknowledged from SNF (NCCR), CTI [Technology Oriented Program (TOP) NANO21], EUCOR Learning and Teaching and Mobility (ELTEM) Nanotechnology project, and the IBM Zurich Research Laboratory.

[1] J. K. Gimzewski, C. Gerber, E. Meyer, and R. R. Schlittler, Chem. Phys. Lett. **217**, 589 (1994).
[2] T. Thundat, R. J. Warmack, G. Y. Chen, and D. P. Allison, Appl. Phys. Lett. **64**, 2894 (1994).
[3] J. Fritz, M. K. Baller, H. P. Lang, H. Rothuizen, P. Vettiger, E. Meyer, H. Guntherodt, C. Gerber, and J. K. Gimzewski, Science **288**, 316 (2000).
[4] R. McKendry *et al.*, Proc. Natl. Acad. Sci. U.S.A. **99**, 9783 (2002).
[5] Y. Arntz, J. D. Seelig, H. P. Lang, J. Zhang, P. Hunziker, J. P. Ramseyer, E. Meyer, M. Hegner, and C. Gerber, Nanotechnology **14**, 86 (2003).
[6] A. Gupta, D. Akin, and R. Basjir, Appl. Phys. Lett. **84**, 1976 (2004).
[7] K. Y. Gfeller, N. Nugaeva, and M. Hegner, Appl. Environ. Microbiol. **71**, 2626 (2005).
[8] B. P. Nelson, T. E. Grimsrud, M. R. Liles, R. M. Goodman, and R. M. Corn, Anal. Chem. **73**, 1 (2001).
[9] K. Bizet, C. Gabrielli, H. Perrot, and J. Therasse, Biosens. Bioelectron. **13**, 259 (1998).
[10] F. M. Battiston, J. P. Ramseyer, H. P. Lang, M. Baller, C. Gerber, J. K. Gimzewisky, E. Meyer, and H.-J. Güntherodt, Sens. Actuators, A **77**, 122 (2001).
[11] B. Alberts, A. Johnson, J. Lewis, M. Raff, K. Roberts, and P. Walter, *The Molecular Biology of the Cell* (Garland Science, New York, 2002), Chap. 15, pp. 852-861.
[12] T. Braun, N. Backmann, A. Bietsch, and M. Hegner (unpublished).
[13] R.-J. Butt, P. Siedle, K. Seifert, K. Fendler, E. Bamberg, K. Goldie, and A. Engel, J. Microsc. **169**, 75 (1993).
[14] G. Y. Chen, R. J. Warmack, T. Thundat, and D. Allison, Rev. Sci. Instrum. **65**, 2532 (1994).
[15] F.-J. Elmer and M. Dreier, J. Appl. Phys. **81**, 7709 (1997).
[16] S. Weigert, M. Dreier, and M. Hegner, Appl. Phys. Lett. **69**, 2834 (1996).
[17] S. Kirstein, M. Mertesdorf, and M. Schönhoff, J. Appl. Phys. **84**, 1782 (1998).
[18] D. Young and R. P. Felgar, Jr., University of Texas Publication No. 44, 1949 (un published), p. 1.
[19] W. Grange, S. Husale, H.-J. Güntherodt, and M. Hegner, Rev. Sci. Instrum. **73**, 2308 (2002).
[20] H.-P. Lang, M. Hegner, and C. Gerber, in *Applied Scanning Probe Methods II*, edited by B. Bhushan and H. Fuchs (Springer-Verlag, Heidelberg, in press).
[21] P. Wagner, P. Kernen, M. Hegner, E. Ungewickell, and G. Semenza, FEBS Lett. **356**, 267 (1994).
[22] P. Wagner, M. Hegner, P. Kernen, F. Zaugg, and G. Semenza, Biophys. J. **70**, 2052 (1996).
[23] M. K. Ghatkesar, V. Barwich, T. Braun, A. H. Bredekamp, U. Drechsler, M. Despont, H.-P. Lang, M. Hegner, and C. Gerber, in *Proceedings of Third IEEE International Conference on Sensors, 2004,*pp. 1060-1063.
[24] W. E. Thomas, L. M. Nilsson, M. Forero, E. V. Sokurenko, and V. Vogel, Mol. Microbiol. **53**, 1545 (2004).
[25] M. Despont, U. Drechsler, R. Yu, H. Pogge, and P. Vettiger, J. Microelectromech. Syst. **13**, 895 (2004).
[26] J. Tamayo, A. D. L. Humphris, M. J. Malloy, and A. M. Miles, Ultramicroscopy **86**, 167 (2001).
[27] X. Su, Y.-J. Wu, R. Robelek, and W. Knoll, Langmuir **21**, 348 (2005).
[28] J. Homola, S. S. Yee, and G. Gauglitz, Sens. Actuators B **54**, 3 (1999).